CHAPTER II
LITERATURE REVIEW

2.1 Transdermal Drug Delivery System (TDDS)

Prausnitz and Langer (2008) reported that TDDS can be divided to three generations. For the first-generation TDDS, they are the transdermal patches using in clinics suitable for delivery of low-molecular weight drugs such as, lipophilic, and efficacious at low doses. Limitation of this generation is the barrier presented by skin's outermost layer, the stratum corneum which is shown in Figure 2.1.

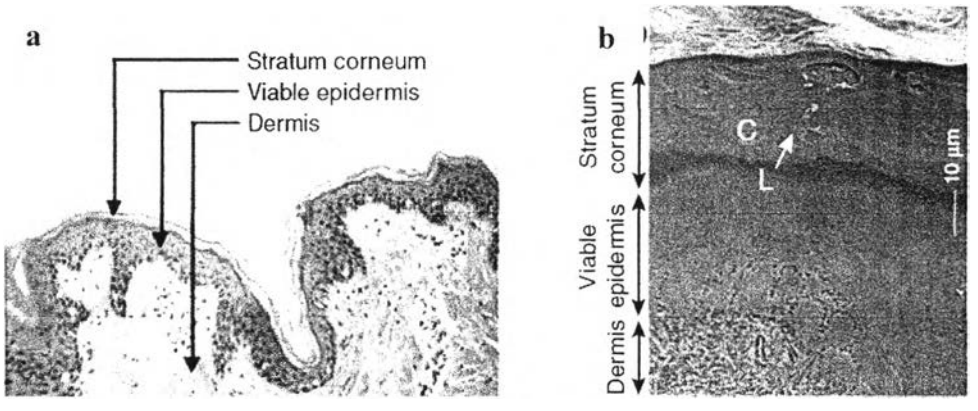

Figure 2.1 (**a**) Skin structure consists of the skin's outermost layer, the stratum corneum, which provides most of skin's barrier properties. The viable epidermis, the second layer, is an epithelial layer that serves to continuously renew the stratum corneum, among other functions. The dermis is a largely fibrous layer that provides skin's mechanical support, as well as the skin's vasculature and anchoring of sweat gland and hair follicle appendages. (Image of H&E stained porcine skin is provided by the courtesy of Samantha Andrews, Georgia Institute of Technology.) (**b**) Stratum corneum structure. Drug penetration across the stratum corneum is primarily limited by the lipids organized in bilayer structures (L) that fill the intercellular spaces between corneocytes (C). Cryo-scanning electron micrograph is provided by the courtesy of Joke Bouwstra, Leiden University and reproduced with permission from Prausnitz and Langer (2008).

The second-generation TDDS have been developed to enhance the skin's permeability. The improvement methods by conventional chemical enhancers, the iontophoresis, and the noncavitational ultrasound through the mechanisms of

1. disturbing stratum corneum structure
2. supplying a driving force for transport into the skin
3. keeping away from harm to deeper, living tissues.

As a result, this generation has higher clinical practice by improving small-molecule delivery for localized, dermatological, cosmetic and some systemic applications, however it has provided little for the delivery of macromolecules.

For the third-generation TDDS, their aim is not only to powerfully disrupt the stratum corneum barrier, but also to protect deeper tissues. Electroporation, microneedles, thermal ablation, microdermabrasion, and cavitational ultrasound are the way to deliver macromolecules and vaccines.

2.1.1 Methods of Controlled Release

2.1.1.1. Temporal control: this method delivers the drug over an extended duration or at a specific time during treatment, which is highly preferred for drugs that are rapidly metabolized and eliminated from the body after organization.

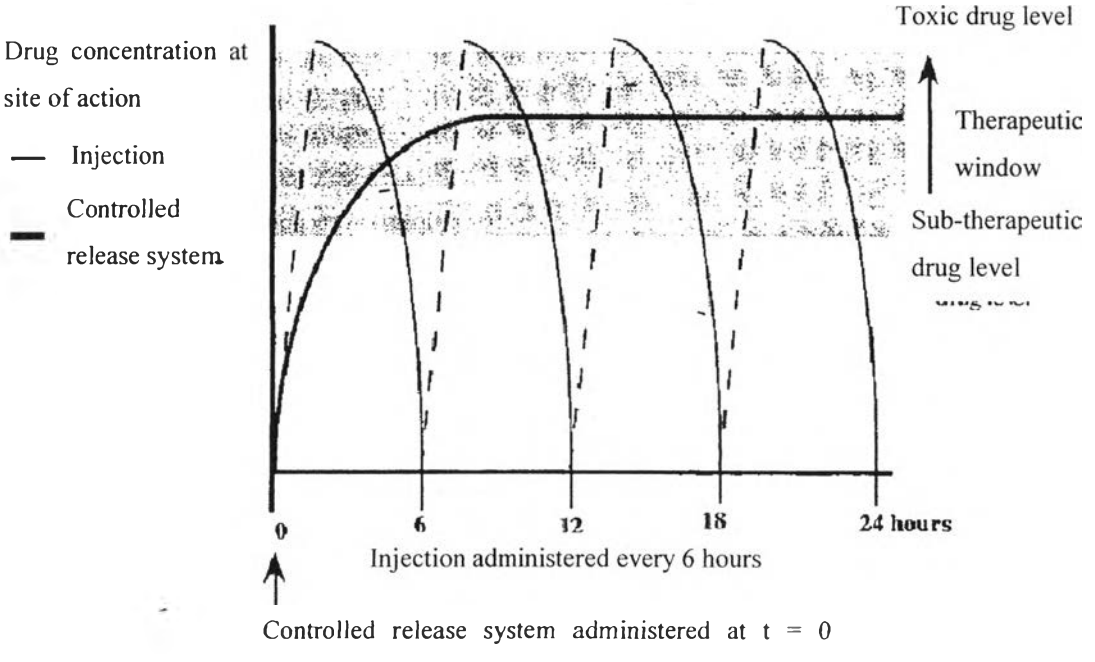

Figure 2.2 Drug concentrations at site of therapeutic action after delivery as an injection (thin line) and as a temporal controlled release system (bold line) (Uhrich *et al.*, 1999).

Figure 2.2 shows the fluctuation of drug concentrations during the 24 h period after injecting the drug and the therapeutic window (i.e., the concentration of drug has no dangerous side effects but gives beneficial effects), which is only a portion of the treatment period. With the controlled release system, the rate of drug release equal the rate of drug elimination so, the drug concentration is in the therapeutic window for the large majority of the observation period (Uhrich *et al.*, 1999).

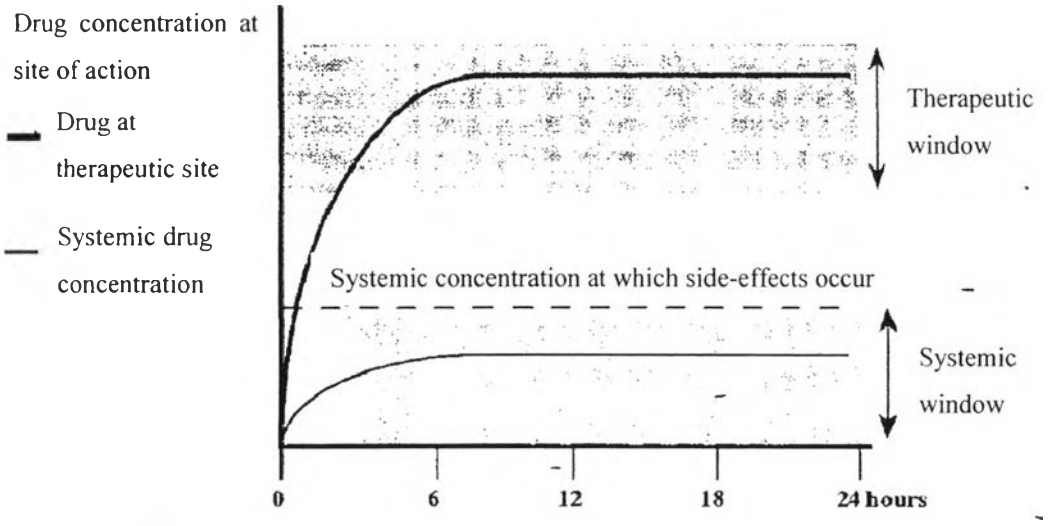

Figure 2.3 Drug delivery from an ideal distribution controlled release system. Bold line: Drug concentrations at site of therapeutic action. Thin line: Systemic levels at which side effects occur (Uhrich *et al.*, 1999).

2.1.1.2. Distribution control: this system is designed to release the drug at the target within the body. Figure 2.3 shows a comparison between drugs concentrations at active site and side-effect production. The distribution control prevents the side effect occurred by a natural distribution and contributes the drug molecules precisely react the target. For example, the drug molecules attack tissues and then cause a side effect by restriction of the further treatment (Uhrich *et al.*, 1999).

2.2 Natural Rubber (NR)

Natural rubber (NR) is one of renewable raw materials obtained from the latex of several plants, but the only important commercial source is the tree *Hevea brasiliensis* which contains 30-35% rubber, namely the polymer named *cis*-1,4-polyisoprene, as shown in Figure 2.4. The latex is stabilized with ammonia after collection and transported to a plant where it is continuously centrifuged to gain higher rubber percentage which is around 60% in rubber content (Geer, 1922).

Sakdapipanich and Rojruthai (2012) reported that the latex is classified by the employed chemicals and processes.

1. High-ammonia (HA) is addition of ammonia which is not less than 0.6% into the latex to have a long-term protection for the concentrated latex.

2. Low-ammonia (LA) includes 0.2-0.3% ammonia, zinc oxide (ZnO), tetramethyl thiuram disulfide (TMTD) as a bactericide, and other necessary additives to preserve concentrated latex.

3. Double centrifuged (DC) is a highly purified latex prepared by recentrifuging the first centrifuged latex to enhance a separation of the non-rubber-components from the rubber. DC latex is generally very stable and has good storage properties.

4. Deproteinized natural rubber (DPNR) is the latex with removed proteins which can cause type I allergic by using a proteolytic enzyme in the presence of surfactants. The physical properties of DPNR are almost equivalent to those of regular NR. Moreover, the dynamic properties are also improved which lead to an increase in the rubber hydrocarbon content.

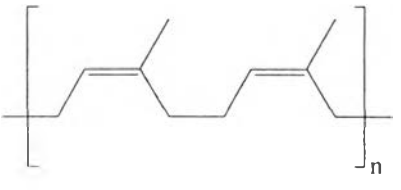

Figure 2.4 The structure of *cis* 1, 4-polyisoprene.

NR has been developed towards improved properties for several decades. Geer, W.C. (1922) studied several developments of the rubber. The rubber products were made up from one or more of thousands of mixtures, each composed of several different substances to give the required physical properties. These substances were made into mixtures by mechanical means, the action of temperature and time, known as vulcanization. To attain highest values, the chemistry of these raw materials, of the vulcanization operation, and of the finished mixtures had been diligently studied during the past few years.

Fanning and Bekkedahl (1951) measured the refractive index of a solution which was consisted of a known weight of acetone-extracted rubber and a known weight of 1-bromonaphthalene to calculate the percentages of rubber hydrocarbon. This method provided results as good as or better than other existing methods, moreover it was simpler and less time-consuming to operate.

Sakota *et al.* (1976) studied the oxidation behavior of styrene-isoprene rubber (SIR) and styrene-butadiene rubber (SBR) using heat aging (70 °C) or UV irradiation (40 °C with a carbon-arc lamp) in air. Copolymers were prepared by the emulsion polymerization and then were observed for the change of gel fraction, the intrinsic viscosity, the molecular weight distribution, and the mechanical properties. SIR mainly occurred through the chain scission and it changed slightly in its mechanical properties upon the presentation of heat. On the other hand, this copolymer occurred through both the chain scission and the crosslinking and had no substantial change in mechanical properties when passing through the UV irradiation. SBR mainly occurred through the crosslinking and sharply became brittle on both oxidation methods.

Adachi *et al.* (1989) irradiated γ-rays to *cis*-polybutadiene in toluene and recently evaluated the swelling behavior of polybutadiene networks (BR) in bulk and in solution of *cis*-polyisoprene (*cis*-PI). They analyzed the behavior based on the Flory-Rehner assumption; they found that the swelling ratio was disproportional to the crosslinking concentration. The absorption ratio increased strongly with decreasing crosslinking concentration and also with decreasing molecular weight of *cis*-PI. Considering the interaction parameter between BR and *cis*-PI which were equal to 0.022 and 0.014 for *cis*-PI, they provided the molecular weights of 2.6×10^3 and 3.16×10^4, respectively. This behavior was attributed to the effect of the repulsive interaction between BR and *cis*-PI.

González *et al.* (2000) observed the mechanism of vulcanization of NR with the sulfurating agent, dipentamethylene thiuram. This study compared the formation of the crosslink precursor in the solutions with and without activators, ZnO and stearic acid, and stated that the reaction followed a similar process. However, the

reaction induction times differed from each other. In addition, the desulfuration reaction was favored by the presence of ZnO.

Phinyocheepand Duangthong (2000) synthesized an epoxidized liquid natural rubber (ELNR) via the reaction of performic acid and a liquid natural rubber (LNR), which was prepared by the degradation of the latex in the phenylhydrazine/O_2 system. Then, photosensitive acrylic acid was added into the ELNR and the progress was tracked by FT-IR spectroscopy. Epoxide ring opening reaction of ELNR at 80 °C completed in a shorter time than the one at 60 °C. In addition, the exothermic heat of photocuring of acrylate double bond of the acrylated ELNR was monitored using a double beam photocalorimeter. The presence of photocleavage initiator (Irgacure 184 and Darocur 1173) and liquid diacrylate monomer (1,6 hexanediol diacrylate and tripropylene glycol diacrylate) promoted the UV crosslinking polymerization. According to the cure kinetics of the elastomers, the rate and extent of the reaction were affected by the diacrylate monomer and photoinitiator concentration.

Durmaz *et al.* (2002) produced series of poly(isobutylene) (PIB) gels using sulfur monochloride as a crosslinking agent. Solution and suspension-crosslinking techniques were used for the preparation of PIB gels in the form of rods, membranes, and beads in the size ranging from 1 to 3 mm. The gels were subjected to dynamic and equilibrium swelling measurements in toluene and cyclohexane as well as to the elasticity tests. Depending on the amounts of sulfur monochloride and butyl rubber in the crosslinking solution, PIB gels with different swelling capacities and elastic moduli were synthesized. The swelling ratio of the gels first rapidly increased with increasing swelling time but then decreased until equilibrium was obtained. This unusual swelling behavior was accompanied with an increase of the elastic moduli of the gels during the swelling process. The results were explained with the post-crosslinking reactions taking place during the swelling process of PIB gels. By using the theory of equilibrium swelling, the number of segments in the network chains and the polymer-solvent interaction parameters were calculated for PIB gels prepared under various reaction conditions.

Bussière *et al.* (2005) used FT-IR spectroscopy, thermoporosimetry, and densitometry to study the photodegradation of polymers including BR, SBR

copolymer, and natural and synthetic PI, under accelerated photo-oxidative conditions. The results, after comparing behaviors of these elastomers with respect to their ability to generate oxidized species, showed the sensitivity of crosslinking of BR-based elastomers was greater than that of PI. Moreover, BR underwent crosslinking reactions early and before the formation of oxidized products, while crosslinking of PI was not detected despite the formation of carbonyl groups during a stimulation period (10-20 h).

Georgoulis *et al.* (2005) investigated the permeation, including breakthrough times, permeation rates, and degree of swelling, of NR, nitrile rubber, and poly(vinyl alcohol) (PVA) glove materials using various solvents. For NR, toluene exhibited higher permeation than methyl ethyl ketone (MEK) which showed that the permeation was proportional to the mixture composition and the degree of swelling. Samples were also exposed to the "low permeation" solvent (LPS) for different time periods prior to a permeation run using the "high permeation" solvent (HPS). The decrease in breakthrough time of the HPS was proportional to the degree of swelling caused by the LPS. Material swelling appeared to control MEK and toluene permeations through the natural rubber.

Choi *et al.* (2006) prepared crosslinked BR fibers using electrospinning and UV irradiation in which 2-methyl-4′-(methylthio)-2-morpholinopropiophenone and trimethylol-propane 3-mercaptopropionate were used as the photoinitiator and the crosslinking agent, respectively. As a result, a cold flow occurred from the very low glass transition temperature (T_g) of BR (below -80 °C), the fiber morphology was not preserved on the uncrosslinked electrospun BR fibers, whereas it appeared on the crosslinked electrospun BR. The crosslink density, tensile strength, modulus, and elongation at break of the electrospun BR fiber were directly proportional to the content of the crosslinking agent. Moreover the crosslinked BR fibers had a higher T_g than the untreated BR.

Chou and Huang (2008) found that for a neoprene rubber the Shore A hardness and tensile modulus were enhanced, whereas their elongation at break, tensile strength, and energy to break were significantly decreased after the exposure to UV irradiation. Furthermore, the storage modulus, loss modulus, and loss factor of

the neoprene rubbers were also influenced by the duration of UV irradiation after examining the dynamic shear properties of the neoprene rubbers before and after exposure to different time periods of UV irradiation.

Riyajan *et al.* (2012) developed a polymer membrane, made of natural rubber-graft-modified cassava starch (NR-g-ST), for controlling a urea fertilizer which can easily degrade in soil. Start with grafting NR with ST, potassium persulfate ($K_2S_2O_8$) was used as a catalyst to supplement hydrophilicity of the rubber. FT-IR spectrophotometer was used to identify the chemical structure of NR-g-ST. TGA gave the thermal stability result where the modified NR-g-ST was higher than that of NR/ST blend. The modified NR was observed for the swelling ratio in water, which decreased as function of ST, while the observed tensile strength was the highest value in the presence of modified ST at 50 phr.

In medical applications, NR and synthetic rubber are interesting materials to use in drug delivery systems and were examined by many researches. Di Colo *et al.* (1986) studied the effect of water-soluble additives on the release of drug from silicone rubber as a matrix. Liquid water carrier including glycerol, ethylene glycol, and polyethylene glycol 200 improved the release of doses from the rubber disks to isotonic phosphate buffer (pH 7.4) without swelling of matrix. The release rate was affected by the drug load, particle size, and on the particular water carrier and water carrier-to-polymer ratio.

Herculano *et al.* (2009) studied a protein delivery from natural rubber latex (NRL) membrane. Bovine Serum Albumin (BSA) was embedded into a latex solution at different polymerization temperatures varying from -10 to 27 °C for controlling the membrane morphology. The results from SEM and AFM microscopy analysis showed various numbers, sizes, and distribution of pores in NRL membranes. While the Lowry Method data showed the protein release was strongly influenced by the morphology of the membrane compared with pore size and number of pores. Moreover, the appropriate polymerization temperature was 27 °C at in which the protein released 66% of its BSA content for up to 18 days.

Al Minnath *et al.* (2011) studied the influence of chemical and physical natures of a thermoplastic polyurethane (TPU)/NR blend film on the transport phenomena. The effect of TPU/NR ratio, temperature, and size of penetrant were

investigated. The equilibrium solvent uptake was inversely proportional to the TPU concentration in the blend. In the diffusion study, the result was compared with various theoretical predictions and showed that the mechanism differed from the normal Fickian trend.

Herculano *et al.* (2011) applied a biocompatible material, NR, as transdermal membrane to deliver metronidazole (MET). X-ray diffraction and FT-IR result demonstrated that MET can be encapsulated without structure and spectroscopic properties change, and also had no molecular-level interaction with NR. In in vitro study, MET in a NR membrane was released faster than in the conventional delivery and experimental conditions controlled the kinetics for specific applications.

Pichayakorn *et al.* (2012) prepared deproteinized natural rubber latex/ hydroxyl-propylmethyl cellulose (DNRL/HPMC) blend films for transdermal nicotine delivery. Due to the mechanical and physicochemical properties, moisture uptake, and swelling ratio of films depended on HPMC and plasticizers so, the composition of each ingredient was verified by FT-IR, XRD, and DSC. The drug release to the skin was controlled without irritation by nicotine matrix films and gave a suitable permeation patterns.

Suksaeree *et al.* (2012) prepared and developed nicotine transdermal patches (NTPs) used for smoking cessation possessing a high efficacy and low cost. DNRL blended with hydroxyl HPMC and dibutylphthalate (DBP) were utilized as matrix membrane for drug delivery and was characterized by FT-IR, XRD, DSC, and SEM. They evaluated the effect of five different types of backing layer on *in vitro* release and skin permeation of NCT. The backing layer could be appropriated and used conveniently in the preparation of NTPs.

Soulas *et al.* (2013) compared two different types of modification applied on silicone rubber (SR) to study the effect on hydrophilicity. There were blending, and addition-grafting reaction between SR and low-molecular weight poly(ethylene glycol). The samples were evaluated as neat films with respect to their water sorption capacity, stability of embedded ethylenoxy groups, mechanical and thermal properties. The blended films showed better results in terms of hydrophilicity, both on surface and in the bulk, whereas the films maintained better mechanical

properties. In term of the release kinetics, blending appeared to offer better possibilities in controlling the drug's release rate through increased water sorption.

2.3 Conductive Polymers

Conductive polymers are materials with a highly π-conjugated polymeric chain. The first evidence of high electrical conductivities in synthetic polymers was in 1977 by preparation of polyacetylene (PA) and eventually (Bagheri *et al.*, 2013). This conjugated structure is also responsible for a strong absorption in the UV-visible range. Although PA was the first reference in this field, this material is not soluble in common organic solvents and not stable under ambient conditions, making it difficult to process and, consequently, inappropriate for electronic devices. Then, in the 1980s, many polymer chemists have developed substituted aromatic polymers to solve the problems of solubility and stability (Morin *et al.*, 2005). Up to now, many conjugated polymers have been intensively investigated, including: poly (*p*-phenylene), poly(p-phenylenevinylene), polythiophene, polypyrrole, polyanilines, polyfluorene, and polycarbazole.

Conductive polymers are applied and utilized in several fields such as thin film transistor, batteries, antistatic coatings, electromagnetic shielding, artificial muscles, light-emitting diodes, gas- and bio-sensors, fuel and solar cells, fillers and corrosion protective coatings, reflecting their necessities and importance. Figure 2.5 shows some repeating units of some general conductive polymers.

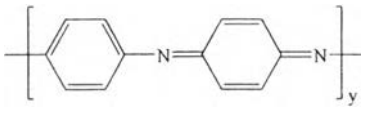

Polyaniline (PANI)

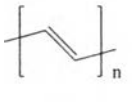

Polyacetylene (PA)

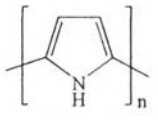

Polypyrrole (PPy)

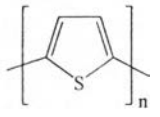

Polythiophene (PT)

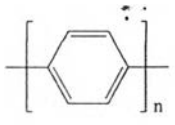

Poly(*p*-phenylene) (PPP)

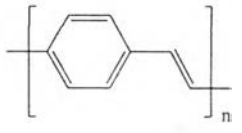

Poly(p-phenylenevinylene) vinylene (PPV)

Figure 2.5 The structure of the common conductive polymers.

In the case of PA the electrical conductivity is produced by placing the alternating carbon-carbon double bond structure directly on the backbone of the polymer. The resonance structure and the mobility of π electrons caused the following electrical conductivity as showed in Figure 2.6.

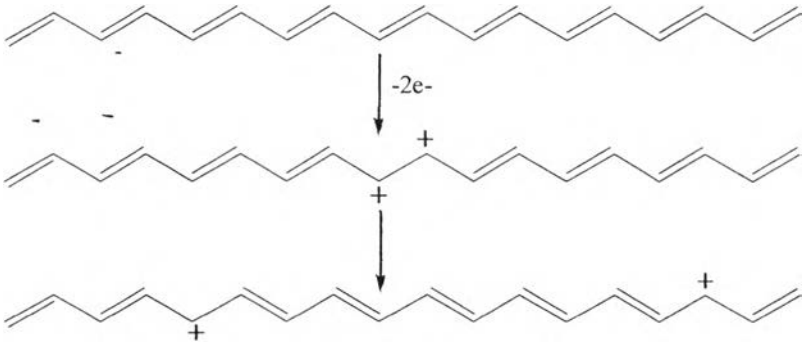

Figure 2.6 Mechanism of electrical conductivity in PA as emblements of CPs.

2.3.1 Conductive Polymer for Drug Release

Sawahata *et al.* (1990) prepared crosslinked poly(methacrylate acid) (PMMA) gel, crosslinked poly(dimethylaminopropylacrylamide) (PDMAPAA) gel, alginic acid gel (Ca-ALG gel), and NaPAA microparticles to study the release of raffinose, pilocarpine hydrochloride (Pil), and insulin by applying electricity. Spectrophotometer or polarimeter was used to detect the amount of released drug as a function of time. The bioactive materials can be released from the gels by the applied electric field which affected the release rate and the amount of released drug.

Ick Chan *et al.* (1991) explored a new controlled drug delivery system to solve the weakness of the conventional system. The polymeric system was consisted of the poly(ethyloxazoline)-poly(methacrylate acid) (PEOx-PMMA) complex and it was studied for the swelling ratio, weight loss, and form changing under applied electric field. The modulated release study of insulin and the extension to other macromolecules showed the drug controlled release could be achieved with this polymeric system.

Fan *et al.* (2008) applied a conducting porous PANI membrane to an iontophoretic TDDS as an electrode using various model drugs of different molecular weights; caffeine, lidocaine HCl, and doxycycline. The study of iontophoresis with PANI|AgCl showed an appropriate permeation which is suitable to practical use. For aqueous-organic partitioning systems, PANI membrane, which was of low porosity, provided lower permeation rates than their hydrophilized polyvinylidene fluoride (PVDF) counterpart membranes.

Chansai *et al.* (2009) blended PPy with poly(acrylic acid) (PAA) film, which was prepared by casting with ethylene glycol dimethacrylate (EGDMA) as a crosslinking agent. The blended films were investigated for the effects of crosslinking ratio and electric field strength on the drug release of PAA and PPy/PAA hydrogels by using a modified Franz-diffusion cell under an acetate buffer of pH 5.5 and at 37 °C, for a period of 48 h. The diffusion coefficient of the drug was calculated using the Higuchi equation, with and without an electric field, at various crosslinking ratios. The drug diffusion coefficient was disproportional to drug size/mesh size ratio, irrespective of the presence of the conductive polymer as the

drug carrier. The diffusion coefficient, at the applied electric field of 1.0 V, became larger by an order of magnitude relative to those without the electric field.

Niamlang and Sirivat (2009) studied the influence of conductive polymer and electric field in TDDS. The apparent diffusion coefficients (D_{app}) and the salicylic acid (SA) release from polyacrylamide (PAAM) hydrogels and PPV/PAAM hydrogels were determined. The D_{app} of both hydrogels obviously obeyed the scaling behavior; $D_{app}/D_0 = (drug\ size/pore\ size)^m$ with the scaling exponent, m, equal to 0.50 at 0.1V. From the results, the combined mechanisms of the expansion of PPV and matrix pore, and the driving force under negative potential, the SA-doped PPV/PAAM provided higher D_{app} than one of the SA-loaded PAAM. In the drug release study, SA used a long time to diffuse through PPV/PAAM in absence of electric field because of the ionic interaction between the anionic drug and the PPV.

Ge *et al.* (2011) explained a new nanoparticle system used for drug delivery with a new temperature and electric field dual-stimulus. Nanoparticles of a conducting polymer (PPy) were loaded with therapeutic pharmaceuticals and were internally localized in vivo with the assistance of a temperature-sensitive hydrogel (PLGA-PEG-PLGA). The release of drug from the conductive nanoparticles was controlled by the application of a weak, external DC electric field. This approach represented a novel interactive drug delivery system that can show an externally tailored release profile with an excellent spatial, temporal, and dosage control.

Bailly *et al.* (2012) synthesized various molecular weights and hydrophobic block lengths of poly((N-vinylpyrrolidone)-block-poly(vinyl acetate)) (PVP-b-PVA) copolymers by controlled radical polymerization. Clofazimine, a water-insoluble drug, was loaded into the PVP-b-PVA vesicles for the drug carrier experiment. They approved the vesicle formation and the aggregation of drug into the vesicle by 1H NMR spectroscopy. The morphology of PVP-b-PVA vesicles was detected by TEM. The data of dynamic light scattering showed that the drug-loaded vesicle size was 180-200 nm with constantly a narrow particle size distribution and it was not proportional to loaded clofazimine. Moreover, the biocompatibility of the PVP-b-PVA drug carrier was confirmed by in vitro experimental results which did not show the cytotoxicity from the polymer vesicle.

Jiang *et al.* (2013) polymerized PPy nanowire electrochemically which was found micro- and nanogaps between the wires by SEM. The gap can be used as reservoir which was appropriate to both hydrophilic and lipophilic drugs. Moreover, their volumes directly influenced to the drug loading capacity. Finally, electrical stimulation (cyclic voltammetry, CV) was used to study the released drug from a protective PPy film. The result showed that the rate of CV and the film thickness affected the amount of drug release.

Sharma *et al.* (2013) prepared 3-dimensionally ordered macroporous PPy-inverse opal thin films via the electropolymerization of PPy through the interstitial voids of a colloidal crystal template composed of PMMA colloids which had a diameter about 430 nm. The risperidone, an antipsychotic drug, was loaded into the PPy inverse opal films, and then entrapped by electropolymerization of a non-porous PPy over layer. SEM and FT-IR spectroscopy provided the data of morphology and chemical composition of the PPy scaffolds, respectively. The result showed that the surface area of PPy inverse opal scaffolds affected the drug loading and releasing capabilities. Moreover, the electrical stimulus was applied to modify drug release profiles with the use of the porous PPy films.

2.3.2 Electrically Stimulated Controlled Release

Juntanon *et al.* (2008) prepared the drug-loaded PVA hydrogels by solution-casting using sulfosalicylic acid and glutaraldehyde as the model drug and the crosslinking agent, respectively. They evaluated properties of the hydrogel including the average molecular weight between crosslinks, the crosslinking density, and the mesh size by Peppas and Merril equation. In the drug release experiment, they used a UV-visible spectrophotometry to examine the amount of released drug. The diffusion coefficients of drug-loaded PVA hydrogels were inversely proportional to crosslink ratio. In addition, the rate of sulfosalicylic acid release was changed and controlled accurately through electric field stimulation as the diffusion coefficients with electric field strength (between 0 and 5 V) as well as on the electrode polarity.

Luo and Cui (2009) proved a drug delivery method by using electricity to control the amount of released drug on sponge-like nanostructured conducting polymer PPy film. They investigated the morphology by SEM images. They succeeded in the controlled release, in which the drugs were loaded within the PPy bulk, and nanoholes, by the electrical stimulation. Moreover, this system was used for the release the multiple drugs because the loaded drug inside nanoholes due to the charge and size of molecules.

Paradee *et al.* (2012) prepared calcium alginate hydrogels (Ca-Alg) using $CaCl_2$ as a crosslinking agent to study the drug release characteristics under an electric field supported TDDS. Benzoic acid and tannic acid were used as anionic model drugs, whereas folic acid was used as a cationic model drug on the Ca-Alg hydrogels. A modified Franz-Diffusion cell with an MES buffer solution of pH 5.5, at a temperature of 37 °C, for 48 h. was used to examine the diffusion coefficients and the release mechanism. They studied on the crosslinking ratio, mesh size, model drug size, drug charge, electric field strength, and electrode polarity. The drug diffusion coefficient was inversely proportional to the crosslinking ratio, and drug size. The drug diffusion coefficient was precisely controlled by an applied electric field and the electrode polarity depending on the drug charge, suitable for a tailor-made transdermal drug delivery system.

Sittiwong *et al.* (2012) fabricated PVA hydrogels via solution casting with various crosslinking ratios using benzoic acid and sulphanilamide as a model drug. They investigated the degree of swelling, the molecular weight between crosslinks, and the mesh size by using a modified Franz diffusion cell at pH of 5.5 and temperature of 37 °C. Crosslinking ratio was inversely proportional to the amount of drug release, the diffusion coefficients, and the mesh size. While, electrostatic force can enhance the drug transportation so, the amount of drug release and the diffusion coefficient increased with increasing electric field strength.

2.4 Polycarbazole (PCz)

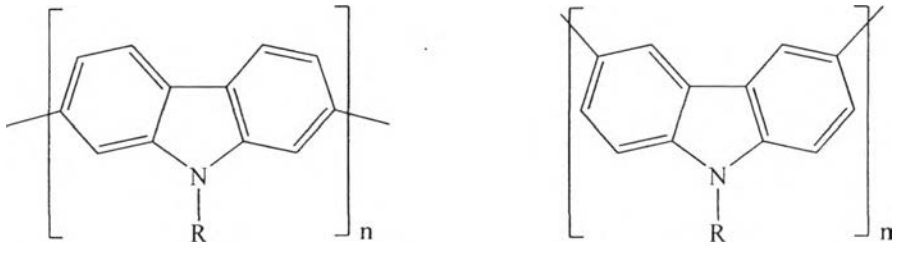

Figure 2.7 The chemical structures for (a) poly (2, 7 carbazole) and (b) poly (3, 6 carbazole).

According to the polymeric structures, the conductive carbazole unit is applicable in photoconductors or charge-transporting materials from the following reasons (Grazulevicius *et al.*, 2003 and Morin *et al.*, 2005).

1. 9H-carbazole is a very cheap starting material readily available from coal-tar distillation.
2. it is a fully aromatic unit providing a better chemical and environmental stability and carbazole-containing compounds exhibit high thermal and photochemical stability.
3. the nitrogen atom can be easily substituted with a wide variety of functional groups to help polymer solubility and to tune the optical and electrical properties.
4. it possesses a bridged biphenyl unit resulting in materials with a lower band gap than traditional PPP.

Furthermore, the carbazole unit can be substituted at different positions, at the 3- and 6- positions and at the 2- and 7-positions which are shown in Figure 2.7, to yield poly (3,6-carbazole) and poly(2,7-carbazole), respectively and provided different properties and potential applications.

Verghese *et al.* (1995) studied the spectrochemical properties and the charge released of PCz films prepared by the electrochemical polymerization on indium-tin oxide-coated glass plates. The experiment was carried out in perchloric acid as a function of pH and oxidation potential (V_{ox}).The UV-visible spectra provided the

peak intensities at 350 and 738 nm at pH $\leq$ 2, while the change on application of the oxidation potential was not be observed in the electronic spectra at 2 < pH $\leq$ 4. The charge release study showed that it reversed with pH on application of a potential difference and a maximum was achieved at pH 3 which demonstrated the complete deprotonation for this conducting polymer.

Verghese *et al.* (1997) measured the electrochemical current response and optical transmittance of an electrochromic cell fabricated using PCz electrochemically deposited onto an indium-tin-oxide (ITO) glass as an anode and platinum as a cathode to investigate the electrochromic properties of PCZ films. Electrochromic displays based on PCz can be fabricated. The long response time was the result from the ionic diffusion process. Whereas the short life cycle of the PCz based electrochromic displays was influenced by either the loss of electroactivity or the dissolution of the film into the solution.

Iraqi and Wataru (2004) synthesized poly(9-alkyl-9*H*-carbazole-3,6- diyl) with palladium catalyzed cross-coupling reactions started with corresponding 3,6-diiodo- and 3,6- dibromo-derivatives. TGA, NMR spectroscopy, and UV-visible and fluorescence spectroscopy were used to characterize including thermal properties of polymer, a range and effect of substituted alkyl group on polymerization, and effect of halogen substituents on the reaction. CV was used to measure the electrochemical properties of the sample. The reaction was only sensitive to the size of substituted alkyl on the monomer. For the result of the electrochemical measurements, materials gave low ionization potentials.

Tamura *et al.* (2009) studied the optical and electrical properties of conjugated polymers containing 3,9- or 2,9-linked carbazole units in the main chain using ethynyl- and iodosubstituted 9-arylenecarbazolylene as a starting material. UV-visible spectra showed the absorption of 3,9-linked, and para-phenylene-linked polymers was around 300 nm, and 350 nm, respectively, whereas meta-phenylene-linked polymers was not observed. For the absorbed light wavelength, the 3,9- linked polymers showed a longer absorbed wavelength than the 2,9-linked polymers which meant they were more largely conjugated than 2,9-linked polymers.

Raj *et al.* (2010) polymerized carbazole in acetonitrile medium using ammonium persulfate as the oxidizing agent. The optimum condition was investigated to procure the better quality and quantity of PCz by choosing solvent, solvent composition, monomer concentration, temperature, polymerization time, and pH. The synthesized PCz was tested with various solvents to examine solubility. UV-visible, FT-IR, 1H-NMR, 13CNMR, COSY, NOESY, and XRD spectroscopy were used to identify, and to characterize the structure of polymer. Moreover, the thermal stability was investigated by DSC and TGA-DTA analysis.

Gupta and Prakash (2010) compared the morphology of PCz synthesized in two different routes. Interfacial polymerization was produced from the reaction of oxidant, ammonium peroxodisulfate, dissolved in hydrochloric acid and a solution of carbazole in dichloromethane. The electrochemical characterization was performed in acetonitrile with 0.5 M tetrabutylammonium perchlorate as supporting electrolyte. CV measured the resulting current at a scan rate 20 mV/s using Ag/AgCl, platinum plate, and platinum disk as reference, counter, and working electrodes, respectively. A voltage was applied in range of -0.2 to 1.6V vs. Ag/AgCl. AFM and SEM micrographs were used to observe the formation and growth of microspheres. The result showed the interfacial polymerization possessed higher crystallinity with spherical morphology.

Naddaka *et al.* (2011) developed a straightforward oxidative liquid phase polymerization (LPP) method for fabrication of spherical functional PCz-based microparticles from corresponding carbazole-containing monomers. SEM was used to identify the morphology. The chemical structure of starting carbazole monomers influenced on the LPP-based microparticle formation.

Qin, R. and Bo, Z. (2012) synthesized a set of monodisperse 2,7-linked carbazole oligomers by using 2,7-dibromo-9-octyl-9H-carbazole as a starting material. DSC and TGA were used to investigate the thermal behavior. The optical and electrochemical properties were observed by UV-visible spectroscopy and CV, respectively. In a solution, the absorption and emission of the 2,7-linked carbazole oligomers was in the UV and in the blue region, respectively, which shifted to longer wavelength with increasing conjugation length. As a film, the shorter oligomers, 3-mer and 5-mer, displayed featureless emission spectra, while the longer oligomers, 7-

mer and 9-mer showed well-resolved emission spectra. The electrochemical results proved that the onset oxidation potentials of oligomers were slightly proportional to the conjugation length.

2.5 Anti-inflammatory Drugs

Anti-inflammatory drugs are usually used to reduce an inflammation as well as other medical conditions that come with it. The main types of anti- inflammatory drugs are glucocorticoids, non-steroidal anti-inflammatory drugs, immune selective anti-inflammatory derivatives, and herbs (Bhondwe, 2011).

2.5.1. Glucocorticoids

Steroids or glucocorticoids can decrease the inflammation by reacting with intracellular receptors, glucocorticoids receptors, which are uniquely shaped. Figure 2.8 shows some of steroids.

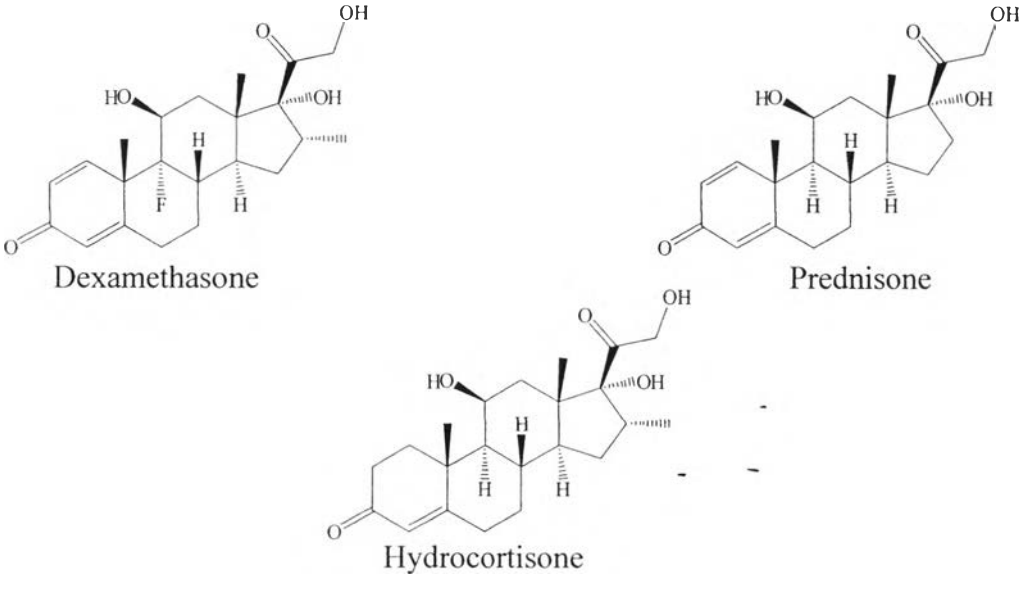

Figure 2.8 The structure of some glucocorticoids.

2.5.2. Non-steroidal anti-inflammatory drugs, NSAIDs

NSAIDs can reduce inflammation by neutralizing cyclooxygenase (COX) enzymes, which promote the synthesis of creating inflammation substances.

There are many common NSAIDs: aspirin, diclofenac, ibuprofen, and indomethacin (Figure 2.9).

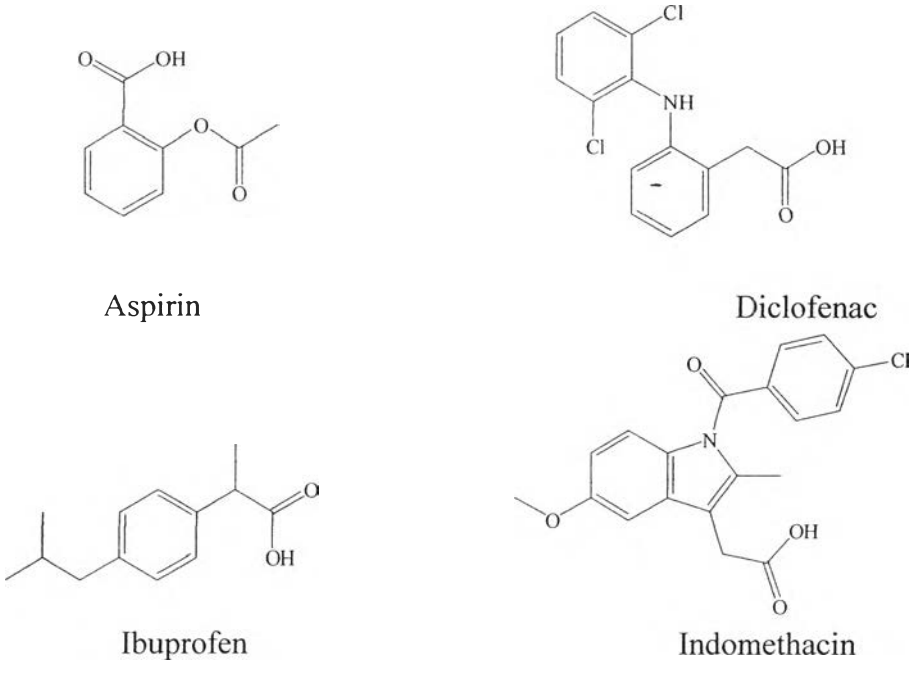

Figure 2.9 The structure of common NSAIDs.

2.5.3. Immune selective anti-inflammatory derivatives, ImSAIDs

ImSAIDs are a class of peptides which are relatively new in medicine. Examples of these peptides are sub-mandibular gland peptide-T (SGP-T), and phenylalanine-glutamate-glycine peptide (FEG). They respond to the inflammation in a different way from glucocorticoids and NSAIDs. ImSAIDs modify the activation of white blood cells in a way that prevents the release of chemicals that generate and increase the inflammatory process.

2.5.4. Herbs

Several herbal extracts are used to reduce inflammation. An extract from willow-bark is the most well-known, aspirin.